https://doi.org/10.37434/tpwj2021.11.04

COMPARISON OF THE PROCESSES OF ELECTROSLAG WELDING AT POWER CONNECTION BY MONO- AND BIFILAR CIRCUITS

Yu.M. Lankin, V.G. Soloviov, V.G. Tyukalov, I.Yu. Romanova

E.O. Paton Electric Welding Institute of the NASU
11 Kazymyr Malevych Str., 03150, Kyiv, Ukraine

ABSTRACT

Electroslag welding (ESW) with wire electrodes with a bifilar circuit of power connection is not applied now. There is every reason to believe that such a connection circuit has even more advantages over the monofilar ESW. Therefore, additional special investigations of the process of bifilar ESW are required. A comparison is given of the process of electroslag welding at power connection by the monofilar circuit and by the bifilar circuit with equalizing wire and doubling of secondary voltage. The results of comparison of both the ESW circuits by energy consumption are given; regularities of heat evolution in the slag pool at the change of its geometrical parameters, coordinates of the points and depth of immersion of the electrodes, value of voltage applied to the electrodes and electrode feed rate were studied.

KEY WORDS: electroslag welding, bifilar circuit, slag pool, metal pool, electric conductivity

INTRODUCTION

Automatic electroslag welding (ESW) is performed with application of one, two, three and more electrode wires. In two-electrode units the electrode wires are connected to the power source in parallel by the electrode–welded item circuit. In 1960ties PWI developed a new process of electroslag remelting (ESR), so-called bifilar electroslag remelting [1–6]. The essence of the method consists in that in a bifilar furnace two consumable electrodes are connected in series to the secondary winding of a single-phase transformer. However, alongside its advantages (such as favourable location of the zones of the main heat evolution in the slag pool, reduction of reactive resistance of the furnace load), the two-electrode furnace turned out to be operational only in a certain range of remelting modes, as a result of ineffective self-regulation, that is electrode melting became unstable at disturbances, acting on the process. To eliminate this drawback with preservation of the advantages of the bifilar circuit, the secondary winding of the power transformer is made with a midpoint, connected to the product being welded by an equalizing wire.

Bifilar ESW with wire electrodes is currently not applied. There is every ground to believe that it has even more advantages over monofilar ESW than in the case of ESR. As the cross-sectional area of consumable electrodes at ESW and ESR differs considerably, the thermophysical processes, causing their melting, also differ essentially. Therefore, additional specialized research of the process of bifilar ESW is required. Such investigations were conducted by mathematical modeling of the processes of two-electrode ESW with the monofilar and bifilar circuit of welding unit connection to ac power source. A circuit of bifilar ESW with an equalizing wire was selected for comparison with the monofilar ESW with the circuit as in Figure 1, *a*. This wire connects the midpoint of the welding transformer secondary winding with the item being welded (Figure 1, *b*).

The objective of this work is comparison of the separate influence of different factors on ESW thermal processes at power connection by the monofilar circuit and by the bifilar circuit with an equalizing wire and doubling the secondary voltage of the power source, by conducting a mathematical experiment.

Figure 1 gives the variants of ESW power circuits.

AD-381Sh unit [7], developed at PWI, was used for physical experiments. Modeling was based on experimental data on ESW with the monofilar power circuit, which were obtained under the laboratory conditions at PWI.

Technological parameters of experimental ESW were as follows: item thickness S = 80 mm; distance between the first electrode and the closest water-cooled shoe $L1$ = 10 mm (at symmetrical arrangement of the electrodes relative to each other); slag pool depth h_{sl} = 50 mm; electrode wire diameter d_{el} = = 3 mm; electrode number n = 2, item from 09G2S; electrode wire from Sv08G2S steel; AN-8 flux; forming shoes from copper. Table 1 gives the data on ESW technological mode.

Results of experimental two-electrode ESW, conducted with the monofilar power circuit, were used for validation of ESW mathematical model. Mathe-

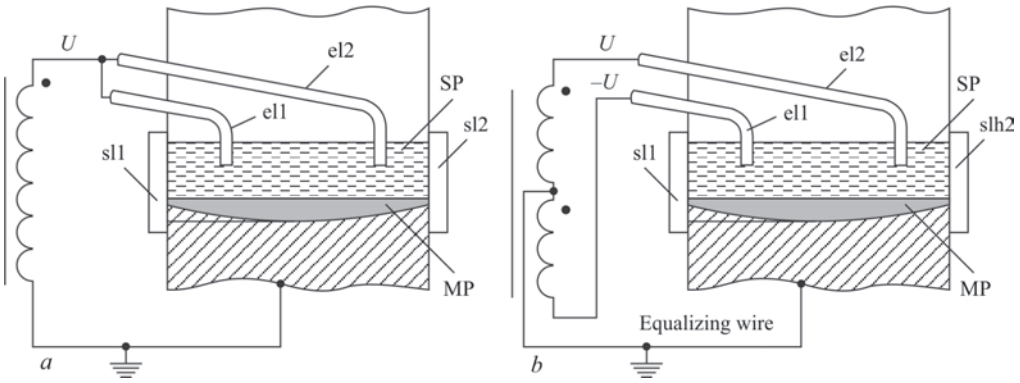

Figure 1. Two-electrode ESW power circuits: *a* — monofilar power circuit; *b* — bifilar power circuit; *U* — power source voltage; el1 and el2 — consumable electrodes; sh1 and sh2 — water-cooled shoes; SP and MP — the slag and metal pool

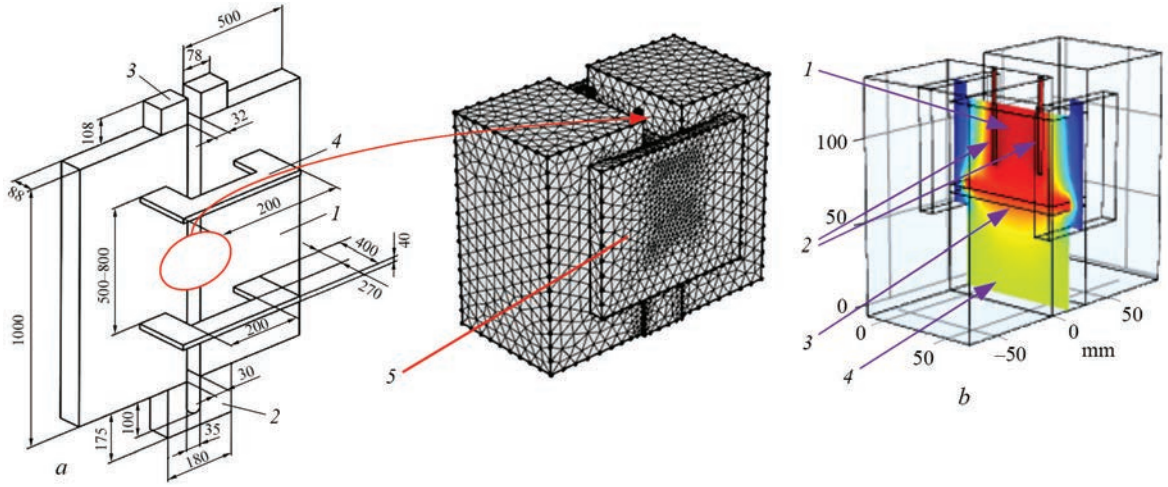

Figure 2. Scheme of assembly of a vertical weld for ESW and finite element model of a fragment of the welding zone (*a*): *1* — item; *2* — inlet pocket; *3* — run-off tap; *4* — cramp; *5* — shoe. Fragment of a graphical model in a section (*b*): *1* — slag pool; *2* — electrodes; *3* — metal pool; *4* — weld

matical modeling was performed on graphical 3D model of a zone of the item region (Figure 2, *a*), which includes the edges of the metal being welded at the depth of 70 mm from both sides, at ~140 mm height, which is adjustable (depending on the specified depth of the slag pool, calculated depth of the metal pool and weld height) and item thickness which is assigned, ~80 mm.

Proceeding from the postulates of the theory of similarity [8], a geometrical model was constructed, which allows for the similarity of its geometrical parameters to those of the physical model. The main condition for modeling was such as to ensure the best correspondence of the geometrical part of the model to the geometrical parameters of the physical experiment, at application of the physical properties of the materials of the slag, item being welded and electrodes [9] (Table 2).

$C\rho[T]$, $\rho[T]$, $k[T]$, $\alpha[T]$, $\sigma_{st}[T]$, $\sigma_{sh}[T]$, parameters were assigned by the respective approximating dependencies (not given in the paper) on temperature T, K. Graphical parameters of the model taken as the base were as follows: S = 80 mm, b = 30 mm, h_m = = 50 mm, d_{el} = 3 mm, $L1$ = 10 mm.

Slag pool heating occurs due to resistive heat of electric current evolving at current flowing through it. The distribution of the electric field, current and potential in the slag pool, item being welded, and the shoes, as well as heat distribution in the volume of the examined zone was studied using its finite element model (Figure 2), consisting of the slag and metal pools, two shoes, two electrodes immersed into the slag pool, as well as fragments of the item and the weld.

Table 1. Data on ESW technological mode

Pass	Welding process	Welding current I, A	Power source voltage U, V	Kind of current	Welding speed v_w, m/h	Electrode wire feed rate v_f, m/h
1	ESW	880–960	38–40	Alt.	1.0	190–210

Table 2. Physical properties of materials used in the model

Parameter	Item	Electrodes	Slag	Shoes	Weld
Heat capacity $C\rho$, J/(kg·K)	$C\rho[T]$	$C\rho[T]$	1400	385	$C\rho[T]$
Relative dielectric permeability ε	1	1	2.5	1	1
Density ρ, kg/m^3	$\rho[T]$	$\rho[T]$	2600	8960	$\rho[T]$
Heat conductivity k, W/(m.K)	$k[T]$	$k[T]$	295	400	$k[T]$
Coefficient of thermal expansion α, 1/K	$\alpha[T]$	$\alpha[T]$	–	17E-6	$\alpha[T]$
Specific electric conductivity σ, S	$\sigma_{st}[T]$	$\sigma_{st}[T]$	$\sigma_{sh}[T]$	6E7	$\sigma_{st}[T]$

The model solves the following equations:

$$\rho(T)C_\rho \frac{\partial T}{\partial t} + \nabla q = Q$$

where $q = -k(T)\nabla T$; Q is the additional heat source (a heated metal pool can be an additional heat source).

When working with stationary electric currents in a medium, which is a conductor, the stationary equation of continuity should be taken into account. In a stationary system of coordinates the point form of Ohm's law indicates that:

$$J = \sigma(T)E,$$

where J is the current density; E is the electric field intensity.

The static form of the continuity equation requires that:

$$\nabla J = -\nabla\sigma(T)\nabla U = 0,$$

where U is the voltage.

After model validation by the results of experimental ESW, the following computation data were obtained at U = 40 V; v_f = 200 m/h:

- total electrode current I = 922 A;
- SP conductivity σ = 11.82 S;
- welding speed of 1.07 m/h.

Such a result practically confirms the correctness of the selected physical and graphical parameters of the model, and enables its application in the planned mathematical experiments. In connection with the fact that model switching from the monofilar to the bifilar power circuit does not change either the physical, or the graphical parameters of the model proper, but changes only the outer power circuits, we assume that the obtained model parameters are also applicable to the model of ESW with a bifilar power circuit.

In the model a stationary problem is solved, and the results of a steady-state process are derived. The model allows determination of the potential, current density and temperature in each point of the studied zone volume at different variations (within ±20 %) of electrode diameter, item thickness, gap width, slag pool depth, as well as electrode immersion depth (within 5–95 % of h_{sl}) and electrode location relative to the shoes (within 10–90 % of S/2).

Mathematical experiment results were used to derive the dependence of specific conductivity of the slag on temperature for each elementary volume of SP. Calculation of the depth of electrode immersion l_{im} in SP (at h_{sl} = 50 mm), as well as average temperature of metal pool surface T_{MP}, depending on U and v_f, was performed. Electrode immersion was determined by the results of calculation of the temperature of the electrode lower edge, which reached that of electrode melting (1500 °C).

Figure 3, *a* shows the dependence of SP conductivity σ on U at unchanged v_f = 280 m/h and $L1$ = 20 mm. SP conductivity at bifilar EBW and equality of consumed power with the monofilar ESW, is always approximately 4 times smaller than that for monofilar variant. The dependence is of an extreme nature. σ maximum is observed at U = 50 V for bifilar ESW and at U = 25 V for the monofilar ESW, respectively.

Figure 3, *b* gives the dependence of I on U. At bifilar ESW the current is always lower, compared to its value with the monofilar circuit, in connection with doubled value of voltage for ESW bifilar circuit. This factor ensures a reduction of energy losses in a short power circuit. Both the dependencies are of an extreme type with a maximum of approximately 480 A at 80 V for bifilar circuit and of approximately 940 A at 40 V for the monofilar circuit.

Figure 3, *c* gives the dependence of ESW consumed power, reduced to a unit of SP volume, on source voltage, U. Both the dependencies are extreme. At the same productivity of ESW for both the power source connection circuits, the consumed power of the process is practically identical.

Presence of extremums of σ (U), $I(U)$ and $P_r(U)$ functions should be used, allowing for optimization of welded joint quality characteristics.

Figure 4 shows the dependencies of SP conductivity, power source current and the reduced consumed power on v_f at U = 100 V for the bifilar circuit and U = 50 V for ESW monofilar power circuit. For all the three dependencies an increase of their values with higher feed rate is observed. The given consumed power of the process is practically the same.

At unchanged low welding voltage and increasing electrode feed rate, the electrode tip moving closer

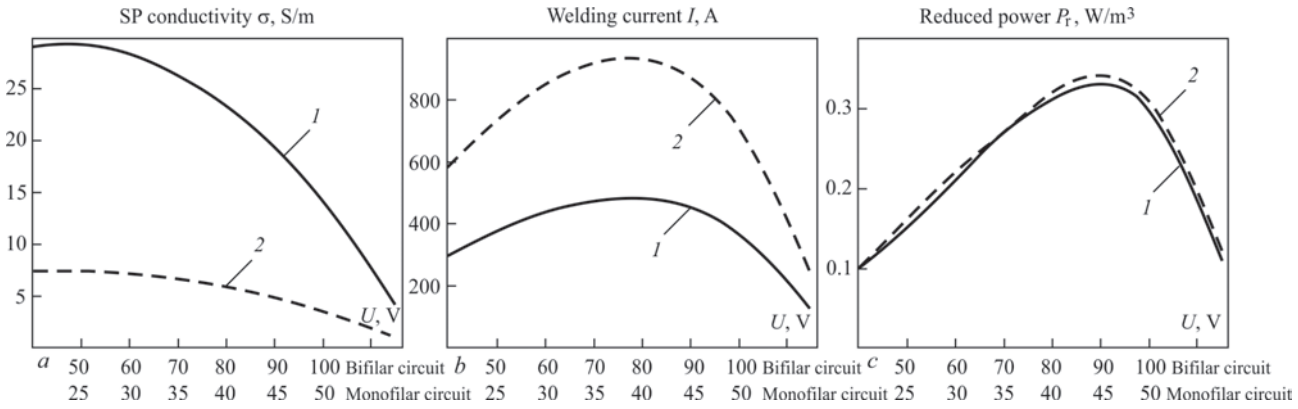

Figure 3. Dependence on voltage U of: *a* — SP conductivity σ; *b* — welding current I; *c* — power P_r reduced to a unit of slag pool volume, for ESW bifilar and monofilar circuits at unchanged v_f = 280 m/h and $L1$ = 20 mm (*1* — ESW bifilar circuit; *2* — monofilar circuit)

to the metal pool, increase of power source current and of the consumed power reduced to SP volume, are usually observed. A reverse process should be observed at lowering of the feed rate. At constant feed rate (for instance, v_f = 280 m/h) and lowering of voltage (for instance, from 80 to 60 V for ESW bifilar circuit or from 40 to 30 V for the monofilar circuit), this regularity becomes reversible (Figure 3, *b*).

Thus, to ensure the set feed rate, at voltage lowering the current should be increased due to deeper immersion of the electrode into SP and reduction of the resistance of the spacing between the electrode and the metal pool. At lowering of the electrodes closer to the metal pool, however, i.e. to the additional heat source, their melting rate becomes higher, while equalizing of the feed rate and linear melting rate occurs without any significant increase of current. This is related to superposition of heat from resistive heating and external heat from the metal pool. Current here decreases and input power is reduced, whereas the melting rate is temporarily stabilized. With time, the thermal level in this zone drops, in connection with reduction of input power (Figure 3, *c*) and electrode immersion becomes deeper. Further lowering of SP temperature may lead to disturbance of ESW stability.

Figure 5 gives the dependencies of SP conductivity, power source current and reduced consumed power on the change of the width of the item gap at unchanged values S = 80 mm, h_{sl} = 50 mm, v_f = 280 m/h, $L1$ = 20 mm, d_{el} = 3 mm, U = 80 V for ESW bifilar circuit and U = 40 V for ESW monofilar power circuit.

At increase of the gap width from 20 up to 45 mm, a reduction of SP conductivity (Figure 5, *a*), lowering of power source current (Figure 5, *b*) and decrease of power (Figure 5, *c*), reduced to a unit of SP volume is observed for both ESW power circuits. This is related to the electrodes moving away from the item. Power (Figure 5, *c*), reduced to a unit of SP volume, practically does not differ for both the power circuits under other equal and unchanged conditions.

Figure 6 gives the dependence of conductivity (Figure 6, *a*), power source current (Figure 6, *b*) and reduced power (Figure 6, *c*) on $L1$. These conditions of the computational experiment are identical to those for Figure 5. At $L1$ increase from 5 to 15 mm a slight decrease in conductivity is observed for both the connection circuits, because of the electrode moving farther from the shoes, which are in direct contact with the item. At $L1$ increase from 15 to 25 mm, a slight increase of conductivity is noted for both the connection circuits, due to electrodes of different polarity moving

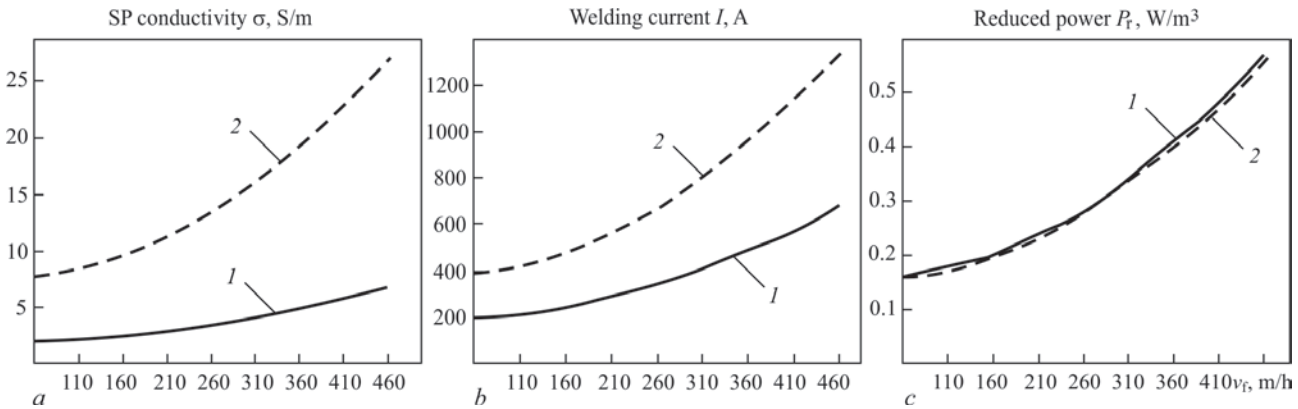

Figure 4. Dependence on electrode feed rate v_f of: *a* — SP conductivity σ; *b* — welding current I; *c* — power P_r reduced to a unit of slag pool volume for ESW bifilar (*1*) and monofilar circuits (*2*)

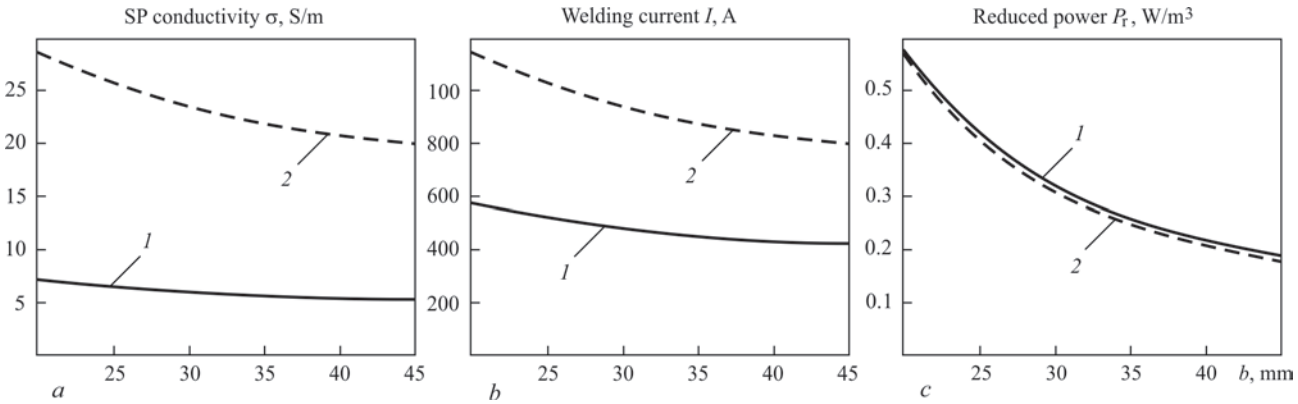

Figure 5. Dependence on welding gap *b* of: *a* — SP conductivity σ; *b* — welding current *I*; *c* — power P_r reduced to a unit of slag pool volume, for ESW bifilar (*1*) and monofilar circuits (*2*)

closer to each other (bifilar circuit) and increase of the slag electrically conducting space (monofilar circuit). At $L1$ increase from 25 to 38 mm, an abrupt increase of conductivity is observed for the bifilar circuit, due to reduction of the distance between electrodes of different polarity and an abrupt lowering of conductivity for the monofilar connection circuit. The latter is related to the fact that the thermal level of SP between the electrodes is increased due to superposition of thermal fields of each of the electrodes. Here the radial component of electrode melting rates becomes greater, electrode immersion becomes smaller to equalize the electrode feed and melting rates, and this, in its turn, leads to current lowering. With bifilar power circuit the electrodes drawing closer together leads to lowering of the resistance between them. The current rises abruptly, thus increasing the radial melting rate, which leads to reduction of electrode immersion. Such a mode may result in one of the electrodes moving out of the slag space. Current changes (Figure 6, *b*) for both the source connection circuits, are of a similar nature. The reduced powers (Figure 6, *c*) for both the circuits practically do not differ at $L1$ increase from 5 to 20 mm. At $L1$ increase from 20 to 38 mm the reduced power in bifilar circuit rises abruptly, and in monofilar circuit it drops abruptly. It is obvious that the electrodes should not be removed from the shoes for more than 20 mm distance, probably $L1 = L/4$.

Figure 7 gives the dependencies of temperature distribution in SP between the middles of the wet portions of both the electrodes at different values of distance L_{el} between them. A comparison of these distributions for both the power circuits was made. One can see from these dependencies that at distance $L_{el} > 27$ mm the SP thermal level between the electrodes is practically the same for both the circuits, i.e. the advantage associated with controlling the item edge penetration by just the voltage in bifilar circuit compared to the monofilar power circuit [1], at ESW is confirmed only at certain electrode spacings.

One of the parameters at ESW modeling, required for controlling the process, which is difficult to measure in real time, is the electrode immersion depth. SP heat, which is the main source for melting at ESW, should be used in the most rational way, both for electrode melting, surface melting of item edges, required interaction of the molten filler metal with the heated slag on the path from the electrodes to the metal pool, and for maintaining the required thermal level and uniformity of metal pool heating. In this connection, for bifilar power circuit particularly important is maintaining the electrode immersion depth at the required level, considering that the heat is mainly concentrated between the electrodes (provided

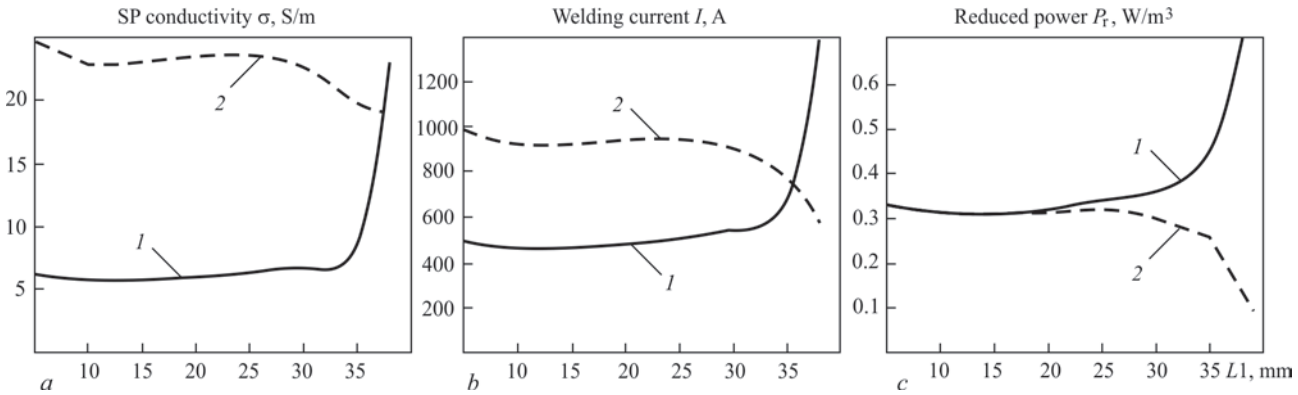

Figure 6. Dependence on the distance between the electrode and shoe $L1$ of: *a* — SP conductivity σ; *b* — welding current *I*; *c* — power P_r reduced to a unit of slag pool volume, for ESW bifilar and monofilar circuits

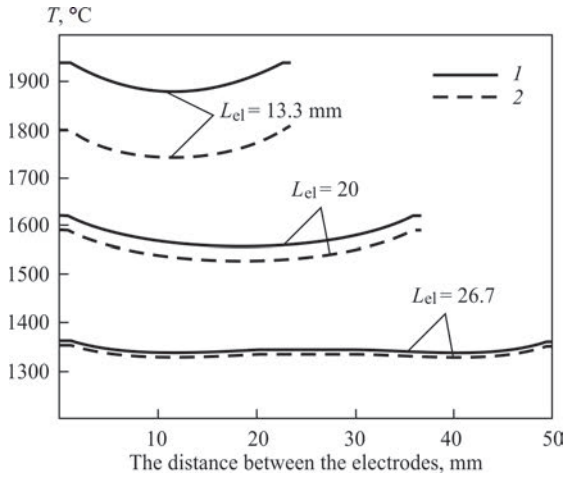

Figure 7. Temperature distribution between the middles of electrode wet parts for both the ESW power connection circuits: *1* — bifilar; *2* — monofilar

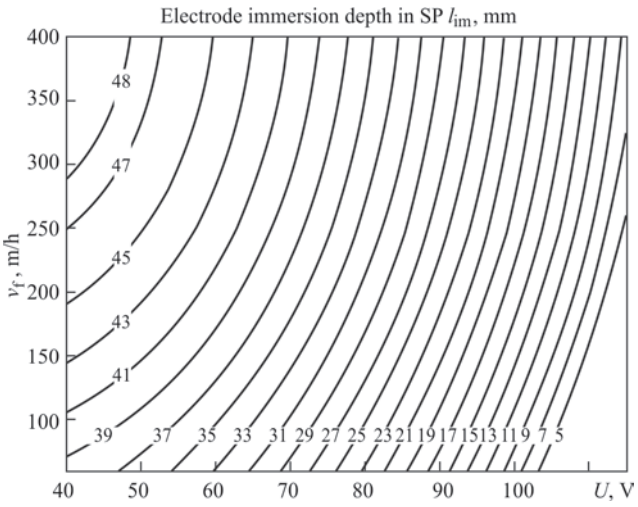

Figure 8. Nomogram of distribution of electrode immersion depth in SP l_{im} at different combinations of U and v_f values for ESW bifilar circuit

the distance between them is sufficient). Figure 8 gives the nomogram of distribution of electrode immersion depth l_{im}, depending on U and v_f, plotted by the results of mathematical experiment on the model and calculation of the temperature of the electrode lower edge until its specified melting temperature has been reached.

The metal pool thermal level is maintained owing to heat and mass exchange between the molten filler metal and the slag pool. Due to convection, the hotter slag conglomerates float upwards, driving the colder ones downwards. As a result of the impact of the gravitational forces the heavier higher-density conglomerates sink to the bottom. As the slag conglomerates move in the magnetic field of electric current, flowing in the electrodes and in SP, through charged ion particles in a certain direction, as well as molten metal drops, moving downwards under the action of gravitational forces, the Ampere electrodynamic force is applied to them.

With the monofilar power circuit, if dc current sources are used, the descending metal drops under the impact of Ampere force will fall closer to the metal pool middle, or will shift to the sides from the metal pool middle, depending on the unit connection polarity. With the bifilar power circuit, if dc current sources are used, the drops will shift from each of the electrodes to the left or to the right, depending on the polarity of the connected power source. At application of ac power source, the drops will descend vertically down along the electrodes, irrespective of whether monofilar or bifilar power circuit is used.

In view the above, the electrode immersion depth with bifilar power circuit should be somewhat increased to ensure the heat balance between SP top and bottom.

Figure 9 shows the nomogram of distribution of the weld form factor ψ, depending on U and v_f. The mathematical experiment was conducted at S = 80 mm, b = 30 mm, h_{sl} = 50 mm, $L1$ = 20 mm, d_{el} = 3 mm.

The best values of the weld form factor are derived at low electrode feed rates and high voltage of the

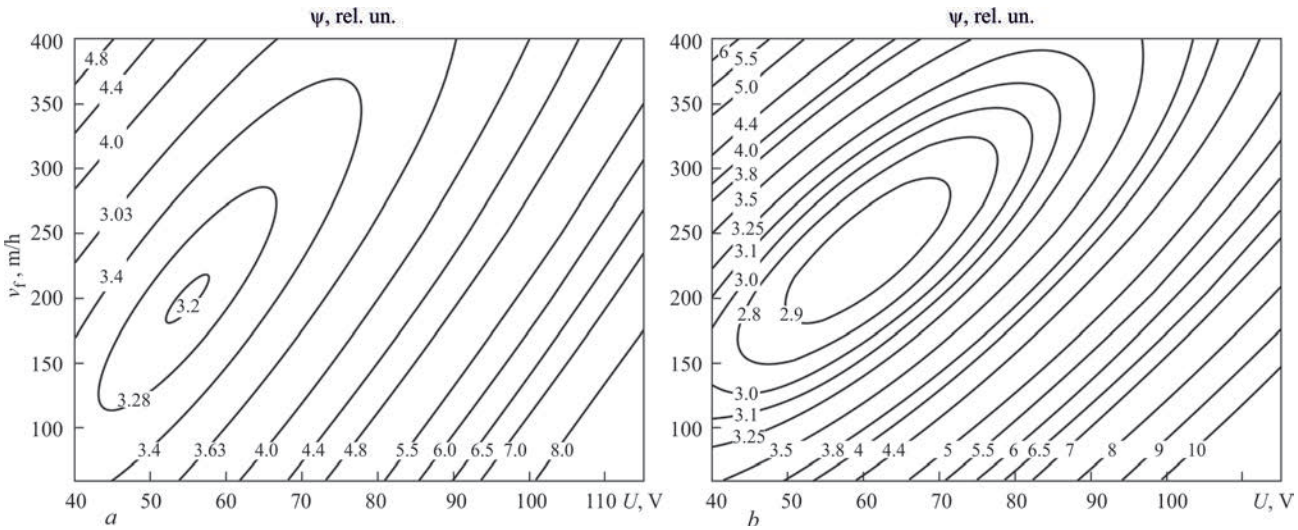

Figure 9. Distribution of values of weld form factor ψ, depending on common values of U and v_f for ESW bifilar (*a*) and monofilar (*b*) power circuits

power source. So, for instance, at v_f = 300 m/h and U = 115 V for bifilar power circuit ψ = 6 and for monofilar circuit ψ = 5.7, i.e. the zone of the modes with a high value of ψ factor is much wider for the bifilar circuit, which allows a more reliable maintenance of the mode with a high weld form factor, and directing the heat flows towards enhancement of the capability for weld surface formation and penetration of the edges being welded.

CONCLUSIONS

1. Searching for slag pool thermophysical parameters, as additional components of ESW model was performed, taking into account the nonuniform temperature distribution in the slag pool, as well as allowing for the influence of the temperature of water-cooled shoes on temperature distribution in the item, and slag and metal pool in the near-boundary regions.

2. Models of ESW with a bifilar and monofilar power circuits were used to perform preliminary comparative study of the regularity of conductivity change in the slag pool at the change of the slag pool geometrical parameters, as well as coordinates of the points and depths of electrode immersion.

3. The advantage associated with controlling the item edge penetration only by voltage with bifilar circuit compared to monofilar power circuit, is confirmed only at certain electrode spacings.

4. The regularity of the change of electrode immersion depth, depending on voltage and electrode feed rate, was studied. It is shown that at electrode edge location near the metal pool, a reduction of electrode immersion depth and of consumed electric power is observed due to superposition of the heat, generated by current flowing in SP, and the MP heat. The resulting heat is sufficient to ensure the required electrode melting rate. However, in connection with the reduction of heat, generated by electric power, in the specified mode, a gradual lowering of the thermal level of ESW process is observed, which may lead to its destabilization.

5. In the general case, the zone of the modes with a high value of weld form factor is much wider for the bifilar circuit than for the monofilar one, which allows a more reliable maintenance of the mode with a rather high weld form factor and directing the heat flows towards enhancement of the capability for weld surface formation and penetration of the edges of items being welded.

REFERENCES

1. Medovar, B.I., Stupak, L.M., Bojko, G.A. et al. (1976) Electroslag furnaces. Ed. by B.E. Paton, B.I. Medovar. Kiev, Naukova Dumka [in Russian].
2. Jing, Xie (2008) Structure advantage of a 5-t double pole series circuit electroslag furnace. *Heavy Casting and Forging*, 5(**3**), 43–45 [in Chinese].
3. Xi-min, Zang, Tian-yu, Qiu, Xin, Deng et al. (2015) Industrial test of a 6-m long bearing steel ingot by electroslag remelting with drawing process. *China Foundry*, 12(**3**), 202–207.
4. Tezuka, M., Yamamoto, S., Takahashi, F. et al. (2014) Internal quality of 2150 mm diameter ingot manufactured using new 150-ton ESR furnace. In: *Proc. of 19th Int. Forgemasters Meeting (IFM). (Tokyo, Japan, 29.09–03.10)*, 90–94.
5. Son, I., Lee, W., Sim, Kw. et al. (2014) Installation of 150-ton new ESR facility and production of 120-ton ESR ingot for 12Cr HIP rotor forgings. *Ibid.*, 333–337.
6. Kubin, M., Scheriau, A., Knabl, M. et al. (2013) Operational experience of large sized ESR plants and attainable quality of ESR ingots with diameter of up to 2600 mm. In: *Proc. of the Int. Symp. on Liquid Metal Processing & Casting (LMPC) (Austin, Texas, USA, 22–25 September)*, 57–64.
7. Lankin, Yu.N., Moskalenko, A.A., Tyukalov, V.G. et al. (2008) Application of electroslag welding in construction and in repair of metallurgical assemblies. *Svarshchik*, **1**, 6–9 [in Russian].
8. Gukhman, A.A. (1973) *Introduction to similarity theory.* 2nd Ed. Moscow, Vysshaya Shkola [in Russian].
9. Sorokin, V.G., Volosnikova, A.V., Vyatkin, S.S. et al. (1989) *Grades of steels and alloys*. Ed. by V.G. Sorokin. Moscow, Mashinostroenie [in Russian].

ORCID

Yu.M. Lankin: 0000-0001-6306-8086,
V.G. Soloviov: 0000-0002-1454-7520,
V.G. Tyukalov: 0000-0003-3491-193X,
I.Yu. Romanova: 0000-0001-7154-1830

CONFLICT OF INTEREST

The Authors declare no conflict of interest

CORRESPONDING AUTHOR

Yu.M. Lankin
E.O. Paton Electric Welding Institute of the NASU
11 Kazymyr Malevych Str., 03150, Kyiv, Ukraine
E-mail: lankin.y.n@gmail.com

SUGGESTED CITATION

Yu.M. Lankin, V.G. Soloviov, V.G. Tyukalov, I.Yu. Romanova (2021) Comparison of the processes of electroslag welding at power connection by mono- and bifilar circuits. *The Paton Welding J.*, **11**, 22–28.
https://doi.org/10.37434/tpwj2021.11.04

JOURNAL HOME PAGE

https://pwj.com.ua/en

Received 13.09.2021
Accepted: 29.11.2021